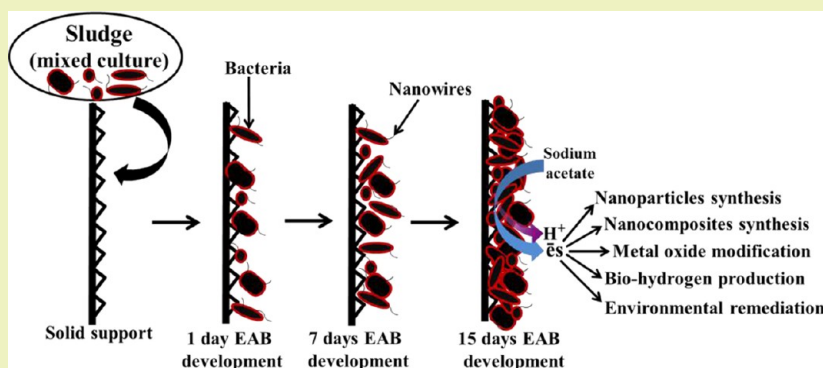


# Mixed Culture Electrochemically Active Biofilms and their Microscopic and Spectroelectrochemical Studies

Mohammad Mansoob Khan, Sajid A. Ansari, Jin-Hyung Lee, Jintae Lee, and Moo Hwan Cho\*

School of Chemical Engineering, Yeungnam University, Gyeongsan-si, Gyeongbuk 712-749, South Korea

## S Supporting Information



**ABSTRACT:** Mixed culture electrochemically active biofilms (EABs) were developed on carbon paper using a sludge with mixed culture bacteria for microscopic and spectroelectrochemical studies because a naturally mixed culture bacterial strain is more applicable than a pure culture strain. EAB development was confirmed by microbial fuel cells (MFCs) by obtaining a constant increase in potential ( $\sim 0.36$  V). Microscopic and spectroscopic studies showed that a mixed culture EABs formed on the support. Cyclic voltammetry (CV), differential pulse voltammetry (DPV), and electrochemical impedance spectroscopy (EIS), which are nondestructive voltammetry techniques, indicated that the EABs could be source of electrons and used effectively for various purposes. Routine *in vivo* analysis of electron transfer between bacterial cells and the electrode was performed, providing insight into the extracellular electron transfer (EET) to the electrode. At low scan rates, CV revealed the catalytic electron transfer ability of EAB between the cells and electrode and showed exceptional redox activities in the presence of acetate. DPV and EIS studies showed that EAB in the presence of acetate can charge the surface by producing and storing sufficient electrons, behave as a capacitor, and have features consistent with EET. Finally, microscopic and spectroelectrochemical studies confirmed the development of a mixed culture EAB and the EET kinetics of EABs. These studies suggest that mixed culture EABs can be used effectively as a biogenic reducing tool for various applications.

**KEYWORDS:** Electrochemically active biofilm, Mixed culture, Biotransformation, Bacteria, Electron transfer, Cyclic voltammetry

## INTRODUCTION

Bioelectrochemical systems (BESs) use living micro-organisms as catalysts in electrochemical reactions. The best known BES is the microbial fuel cell (MFC), which is a device using metal-respiring bacteria to convert the chemical energy of substrates dissolved in wastewater to electrical energy.<sup>1</sup> BESs allow electricity generation from wastewater, electricity-driven bioproduction, bioremediation, and biosensing.<sup>2,3</sup> Many of these processes are quite promising. On the other hand, to date, the performance of bioproduction processes is not yet at the level needed for practical applications because it is critical for enabling high catalytic activity of the electrochemically active microorganisms (EAMs). Effective electron transfer and high process performance needs to be achieved regardless of whether the biocatalyst exists as a planktonic cell, a monolayer cell surface, or a fully developed biofilm.<sup>1–3</sup> On the other hand, despite the many different approaches and extensive research, many questions regarding the functioning of EAMs remain

unanswered. This is certainly due to the complexity of bioelectrochemical processes because they depend on microbial, electrochemical, physicochemical, and operational considerations. This versatility and complexity calls for a variety of analytical tools to study mixed culture-derived electrochemically active biofilms (EABs).<sup>1–4</sup>

Bacteria, which forms a multilayered aggregation (i.e., a microbial biofilm) attached to the electrode, transfer the electrons derived from oxidation of the substrate (waste or organic matter) to the electrode. The ability of metal-respiring bacteria to reduce insoluble electron acceptors that cannot enter the cell (e.g., electrodes) requires an efficient extracellular electron transfer (EET) tool shuttling electrons across the outer membrane of the microbial cell to the electrode.<sup>3–5</sup> A

**Received:** September 1, 2013

**Revised:** November 6, 2013

**Published:** November 19, 2013

range of EET mechanisms from bacteria to the anode is suggested, such as indirect transfer using electron shuttling proteins (e.g., cytochromes) or low molecular weight electron shuttles (e.g., mediators), via electron conducting “nanowires” (pili) produced by the bacteria or direct EET from the cell surface redox active proteins.<sup>3</sup> Understanding the mechanism of EET through electroactive microbial biofilms is a challenge in fundamental and applied life sciences. To date, electrochemical techniques, such as cyclic voltammetry (CV), have been applied successfully to examine EET process in intact and viable microbial biofilms on electrodes, providing important insight into their redox properties.<sup>3–7</sup> Unfortunately, CV alone cannot provide complete insight into the mechanisms involved in the redox processes. On the other hand, coupling CV with differential pulse voltammetry (DPV) and electrochemical impedance spectroscopy (EIS) and spectroscopic techniques overcome these limitations.<sup>1–7</sup> These approaches, which have often been used to study isolated proteins and enzymes attached to electrodes, are also applicable for examining EABs. The ability of certain microorganisms to connect their metabolisms directly to an external electrical power supply is very exciting, and extensive research on the possibilities of EABs applications is ongoing.<sup>4–7</sup> The best known application of EAB is possibly the MFC, which can convert biomass into electrical energy. Nevertheless, EABs coated onto electrodes have recently become popular in other fields, such as the biosynthesis, bioremediation, and biosensor design.<sup>1–7</sup>

Recently, mixed culture EABs was reported to be a biogenic reducing tool for the synthesis of nanoparticles (Au, Ag, and Cys–Ag),<sup>8–10</sup> nanocomposites (Au@TiO<sub>2</sub> and Ag@TiO<sub>2</sub>),<sup>11–13</sup> band gap narrowing (TiO<sub>2</sub> and ZnO)<sup>14,15</sup> and biohydrogen production,<sup>16</sup> which is novel, simple, and green. The advantage of these protocols is that the use of mixed culture EABs as a reducing tool does not involve external energy input, toxic chemicals or expensive solvents. In addition, the reactions take place at room temperature, which makes the synthesis of nanoparticles and nanocomposites highly suitable and efficient in the field of nanoscience.<sup>8–16</sup> Therefore, mixed culture EABs were examined further using a range of techniques to better understand the biogenic reducing behavior and other characteristics.

This paper presents an overview of the parameters defining the developments of EABs and the analytical tools to examine the EABs at different levels. To the best of the author’s knowledge, this is the first report to include a wide range of techniques, such as microscopic, spectroscopic, electrochemical (CV, DPV, and EIS) and MFC to study, understand, standardize, and characterize the mixed culture EABs. This will further strengthen the field of BESs and the use of mixed culture EABs in nanomaterial syntheses, band gap narrowing of metal oxides, biohydrogen production, and bioremediation. Therefore, a standardized framework appears essential. Recently, few of our previously reported studies proposed a novel and optimized approach to develop mixed culture EABs outside MFC for different purposes.<sup>8–16</sup> This approach produced high performance mixed culture EABs for nanomaterial syntheses that were considerably faster and easier to handle, even for the nonprofessionals. The present report shows how these approaches have provided important complementary information to those obtained by electrochemical methods, i.e., information on the electron transfer kinetics.<sup>1,2,17,18</sup> This study will also show that the biocatalytic activities of EABs depend mainly on biofilm

formation on the support and substrate (organic matter or waste) used. This study was not intended to examine the microbe–electrode material interaction, type of bacteria, or strain, which might be the scope of a further study.

## ■ EXPERIMENTAL SECTION

**Materials.** Sodium acetate (CH<sub>3</sub>COONa), NaCl, sodium phosphate monobasic (NaH<sub>2</sub>PO<sub>4</sub>), and sodium phosphate dibasic (Na<sub>2</sub>HPO<sub>4</sub>) were obtained from Duksan Pure Chemicals Co. Ltd. South Korea. Carbon paper (without wet-proof) and Pt-coated carbon paper (0.5 mg Pt/cm<sup>2</sup>) were purchased from Fuel Cell Earth LLC Co., USA. Nylon membrane fiber filter (0.45 μm) was obtained from Whatman, Germany. All the other chemicals used in this study were of analytical grade and used as received. All solutions were prepared using deionized water prepared using a PURE ROUP 30 water purification system.

**Methods.** Electrochemical experiments, such as CV, differential pulse voltammetry (DPV), and electrochemical impedance spectroscopy (EIS), were conducted on a potentiostat (VersaSTAT 3, AMETEK, USA) using Ag/AgCl (saturated with KCl) as the reference electrode, Pt gauze as the counter electrode, and EABs on carbon paper and carbon paper only as the working electrode in 50 mL, 0.1 M phosphate buffer solution (pH 7; 0.1% NaCl) as the supporting electrolyte at room temperature. EIS was performed in a 1 mM K<sub>3</sub>[Fe(CN)<sub>6</sub>] and K<sub>4</sub>[Fe(CN)<sub>6</sub>] solution. The electronic absorption/reflectance spectra (UV–vis spectra) of EABs were obtained using an UV–vis–NIR double beam spectrophotometer (VARIAN, Cary 5000, USA) equipped with a diffuse absorbance/reflectance accessory. EAB was placed in a sample holder that was then placed at the integrating sphere for the absorbance measurements. X-ray diffraction (XRD, PANalytical, X’pert PRO-MPD, Netherlands) was performed using Cu Kα radiation (λ = 0.15406 nm) and a diffraction angles ranging from 10° to 90°. The surface morphology of the EABs was observed by scanning electron microscopy (SEM; Hitachi S-4100, Japan). The morphology of the nanomaterials was examined by transmission electron microscopy (TEM, Tecnai G2 F20, FEI, USA) operating at an accelerating voltage of 200 kV. The potential generated by the MFC was recorded using a digital multimeter (Agilent 34405A, USA) connected to a computer.

**Media, Inoculum, Preparation of EABs, and Their Optimization in MFC.** Primary sludge was collected from a Biogas plant (Paju, South Korea). The chemical oxygen demand (COD) of the sludge was 1200 mg L<sup>-1</sup>. The sludge served as a mixed culture bacterial inoculum for the formation of mixed culture EABs on carbon paper and nylon fiber. EABs on carbon paper and nylon fiber were made, as reported earlier.<sup>8–16</sup> The EABs were developed in two different ways. In the first way, in a 200 mL mineral salt medium, 0.2 g sodium acetate was added as a substrate.<sup>19</sup> Subsequently, 10 mL of the anaerobic sludge was added and N<sub>2</sub> gas was sparged for 5 min to create anaerobic conditions. Finally, carbon paper and nylon fiber (2.5 cm × 4.5 cm) were dipped separately in the bottle and the bottle was sealed. All media, including the bacterial inoculum, were changed every two days under anaerobic conditions. This was repeated for two weeks. Suitable mixed culture EABs that formed on the carbon paper (Figures 1 and 2) were examined and confirmed using MFC by obtaining the appropriate voltage. The mixed culture EAB formed on the nylon fiber was used only for comparative XRD and UV–vis spectroscopy because nylon fiber is nonconducting. In the second way, EAB on carbon paper was also prepared in the MFC anode, as reported earlier for comparative studies.<sup>19,20</sup>

To examine the uniform and appropriate development of biofilms on carbon paper, the as-prepared EABs were monitored in the MFC anode to record the optimum voltage using a multimeter. The MFC consisted of two identical chambers (anode and cathode chamber) separated by a Nafion membrane. Each chamber had an effective volume of 250 mL. The bottles were connected by two clamps between the flattened ends of the two glass tubes (inner diameter = 1.3 cm) fitted with rubber gaskets. In the anode chamber, an EAB was developed on plain carbon paper (2.5 cm × 4.5 cm) in artificial

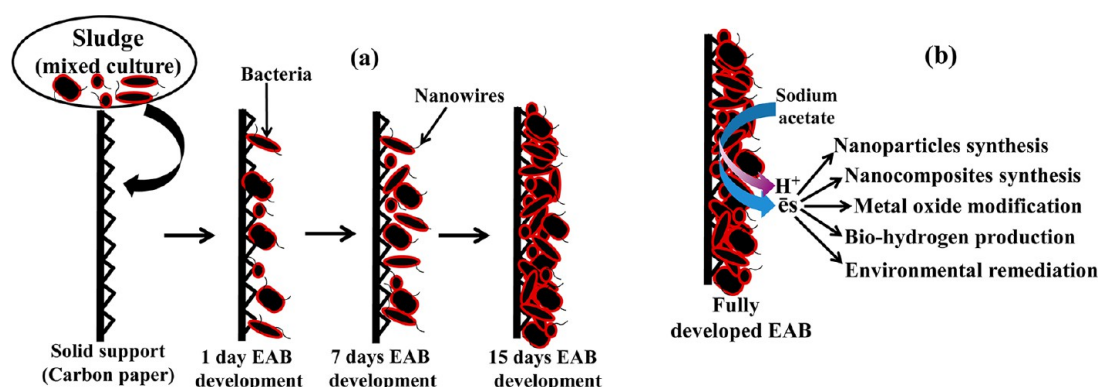


**Figure 1.** (a) Proposed mechanism for the development of mixed culture EABs and (b) biological decomposition of acetate and electron transfer for the nanomaterial synthesis, metal oxide modification, biohydrogen production, and environmental remediation.

wastewater using sodium acetate as the electron donor ( $1 \text{ g L}^{-1}$ ). A mineral salt medium was added to the anode chamber and inoculated with 10 mL of the anaerobic sludge.<sup>19</sup> The anode chamber was bubbled with nitrogen for 10 min to remove oxygen (anode pH  $\sim 7.4$ ). Initially, a conventional H-type MFC was operated to obtain an efficient MFC system for the experiment using Pt coated carbon paper as the cathode electrode.<sup>19,20</sup> The cathode chamber was filled with a phosphate buffer solution (50 mM, pH 7) and bubbled continuously with air. After 1 day of continuous operation, the MFC produced a stable power density of  $40 \text{ mW/m}^2$ , which corresponds to previous results.<sup>20</sup> During EAB development, the MFC was connected to a resistance box at  $1000 \Omega$  and run at  $30^\circ \text{C}$  under atmospheric pressure. The potential obtained in this study refers to biofilms formed on carbon paper for different times (1–15 days). The same biofilm was used for 15 days to continue the growth of the biofilm and then measure the potential. The above-mentioned mixed culture EABs, which was developed outside the MFC, was tested in the MFC anode after 1, 7, and 15 days to confirm the EAB growth by monitoring the potential.

The living mixed culture EABs formed on carbon paper outside the MFC was used for different spectroscopic, electrochemical and morphological studies, whereas the EAB formed on the nylon fiber was used for a comparative XRD and UV–vis spectroscopy only.

**Pretreatment of EABs for SEM.** The morphology of EAB was examined by SEM after pretreating the EAB formed on carbon paper and nylon fiber using the following modified protocol.<sup>21,22</sup> Briefly, EAB formed on carbon paper and nylon fiber were fixed directly by adding glutaraldehyde (2.5% final) and formaldehyde (2% final) and incubated at  $4^\circ \text{C}$  overnight. Postfixation was performed for 90 min with an osmium tetroxide solution (containing 3 mL of sodium phosphate buffer 0.2 M, 3 mL of 2%  $\text{OsO}_4$  and 3 mL deionized water). Further, the EAB was washed and dehydrated by successive 10 min incubations in 50% ethanol, 70% ethanol, 80% ethanol, 90% ethanol, and 95% ethanol followed by two successive 20 min incubations in 100% ethanol. After dehydration, the EAB was incubated in isoamyl acetate for 20 min and dried with a critical-point dryer (HCP-2, Hitachi, Japan). The pretreated EABs were affixed to the SEM stubs and coated with platinum for 200 s using an ion-sputter (E-1030, Hitachi, Japan). The specimens were examined by SEM. The voltage was set to 15 kV and viewed at a magnification from  $\times 2000$  to  $\times 20\,000$ .

**Electrochemical Studies (CV, DPV, and EIS) of the Mixed Culture EABs.** Electrochemical studies (CV, DPV, and EIS) were used for different spectral responses, such as the redox response of the carbon source, EET, and growth of EABs, which highlight the potential use of these techniques for examining the redox electrochemistry of living mixed culture EABs. The electrochemical measurements (CV, DPV, and EIS) of EABs developed on carbon paper for 1, 7, and 15 days, and carbon paper only with and without acetate were performed with a computer-controlled potentiostat (VersaSTAT 3, USA) with a three electrode arrangement. The EABs developed on carbon paper for 1, 7, and 15 days were used as the working electrode, platinum

gauze as the counter electrode, and an Ag/AgCl electrode (saturated with KCl) as the reference electrode. All the experiments were performed anaerobically at  $30^\circ \text{C}$  in succession without stirring. Here, all the electrode potentials referenced to Ag/AgCl (saturated with KCl).

CV was performed at a scan rate of  $1 \text{ mV s}^{-1}$  versus Ag/AgCl (saturated with KCl). The parameters for DPV were as follows:  $E_{\text{initial}} (E_i) = 0.08 \text{ V}$  versus Ag/AgCl; pulse height = 50 mV; pulse width = 500 ms; step height = 2 mV; step time = 500 ms; scan rate =  $4 \text{ mV s}^{-1}$ . The EIS experiments were performed for the EABs developed on 1, 7, and 15 days with and without acetate in a 1 mM  $\text{K}_3[\text{Fe}(\text{CN})_6]$  and  $\text{K}_4[\text{Fe}(\text{CN})_6]$  solution, maintaining a direct current voltage between the working electrode and reference electrode (potentiostatic EIS) because the electron transfer processes by EAB were observed to be voltage dependent.<sup>23</sup> EIS was performed at 0.0 V versus Ag/AgCl (saturated with KCl), and the frequency was fixed from  $10^4$  to 1 Hz with an amplitude of 10 mV because most biological charge transfer phenomena are observed in this range.<sup>24</sup> EIS was typically performed only at the end when the CV and DPV measurements were over after a long period of time. All the experiments were performed as independent bioelectrochemical triplicates for a total duration of approximately 3 months.

## RESULTS AND DISCUSSION

**Electrochemically Active Biofilms.** Electrochemically active biofilms (EABs) are well-known in microbial fuel cells that produce electrons and protons.<sup>1–7,17,18,25</sup> Recently, our group has started using mixed culture EABs as a biogenic reducing tool for the synthesis of different types of nanoparticles (Au, Ag and, Cys–Ag),<sup>8–10</sup> nanocomposites (Au@ $\text{TiO}_2$  and Ag@ $\text{TiO}_2$ ),<sup>11–13</sup> band gap narrowing of metal oxides,<sup>14,15</sup> biohydrogen production,<sup>16</sup> and bioremediation.<sup>20,25–27</sup> The use of a mixed culture EAB is more practical than a pure culture (single strain) because, in nature, microbial communities are a mixed culture and the use of a pure culture is inconvenient, cumbersome, and limited.<sup>26–31</sup> Mixed culture EABs effectively oxidize organic substrates, such as acetate to electrons, protons, and  $\text{CO}_2$  without combustion. The above-mentioned synthetic protocols are novel, green, and biogenic. In addition, they utilize the biologically produced electrons and protons and do not involve any external energy input, which makes the syntheses of nanoparticles, nanocomposites, biohydrogen production, and bioremediation highly useful and efficient in the field of nanomaterial syntheses, sustainable energy, and environmental remediation.<sup>8–16,25–27</sup> Furthermore, other highly sensational observations are that these processes do not contaminate the products, comprise any harmful chemicals, capping or reducing agents, and severe treatments.



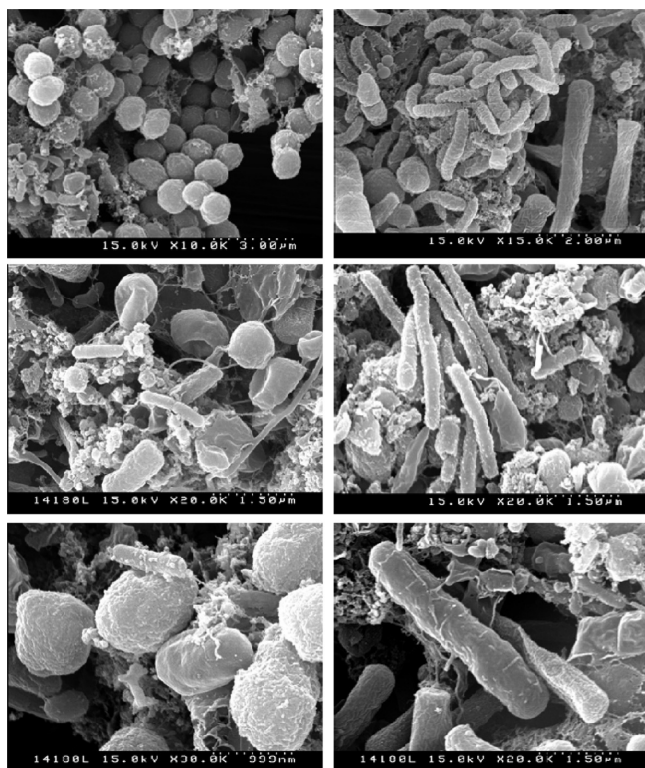


**Figure 2.** SEM images (different magnifications) of the mixed culture EABs developed on carbon paper for 15 days.

The entire process takes place in water at room temperature which shows the importance of EABs. Figure 1a shows the proposed mechanism for the development of mixed culture EABs outside the MFC, whereas Figure 1b shows the synthesis and modification of nanomaterials, biohydrogen production, and environmental remediation by EABs, which is simple, easy, and environmentally friendly. In these processes, which were reported previously, mixed culture EABs were exploited as a biogenic reducing tool that provides an excess of electrons and protons by biologically decomposing sodium acetate.<sup>19,20,32</sup> Figure S1 (Supporting Information) shows TEM images of gold nanoparticles, Au@TiO<sub>2</sub> nanocomposites, and Ag@TiO<sub>2</sub> nanocomposites synthesized by mixed culture EABs as a biogenic reducing tool for different purposes.<sup>10–12</sup>

#### Mechanism for Mixed Culture EAB Development and Electron Transfer. Morphological Study of Mixed Culture

EABs. The surface morphology of the mixed culture EABs were observed by SEM, which clearly shows that EABs consisted of different types of bacteria (Figure 2). The bacteria on the biofilm were a mixed culture, which may include different types of bacteria that vary in morphology from spherical, rod, and oval shape. Bacteria, such as spherical and rod shape, shows the presence of nanowires (pili), which can be responsible for extracellular electron transfer (EET).<sup>29</sup> The electrons generated by bacteria upon the oxidation of acetate could be transported effectively by these nanowires to an electrode during different electrochemical and biocatalytic reactions.<sup>2,29–35</sup> A recent model proposed that electrons are transported via pili, which possess delocalized electronic states to function as protein wires with metallic-like conductivity, without the involvement of c-type cytochromes (c-Cyts).<sup>33–35</sup> These living wires (nanowires) can provide direct extracellular electron exchange for bioenergy, bioremediation and biosynthesis.<sup>8–16,36</sup> In previous reports, mixed culture EABs were exploited for the synthesis of different metal nanoparticles, nanocomposites, and biohydrogen production,<sup>8–16,25,26</sup> where these nanowires (pili) could have played an important role in EET from bacteria to metal ions or metal oxides. Figure S3 and S4 (Supporting Information) show low magnification SEM images of mixed culture EABs developed on carbon paper for 7 and 15 days; whereas Figure S5 (Supporting Information) shows SEM images of mixed culture EABs developed on nylon fiber for 15 days.

**UV–visible Spectra of EABs.** UV–vis spectroscopy (DRS) is a desirable method for examining the biological mass on biofilms.<sup>1,2,7,37–40</sup> The heme entities in c-type cytochromes (c-Cyts) showed high molar absorption in the visible range, thereby making visible absorption a simple and effective tool for studying the in vivo behavior of EABs.<sup>39,40</sup> Therefore, DRS was used to analyze the redox state of the c-Cyts absorption of EABs. Figure 3a and b shows the electronic absorbance spectra of EABs formed for 15 days on carbon paper and nylon fiber, respectively. Supporting Information Figure S2a and b shows the reflectance spectra of EABs formed for 15 days on carbon paper and nylon fiber, respectively. Two different supports were chosen to observe the development of EABs because both supports have different porosity, which might affect EAB development. From the spectra (Figure 3a and b), it is clear that the absorbance increased significantly after the formation of EAB on carbon paper and nylon fiber, which shows the growth of the EABs on the different type of supports. The growth of EAB on carbon paper was much better than nylon

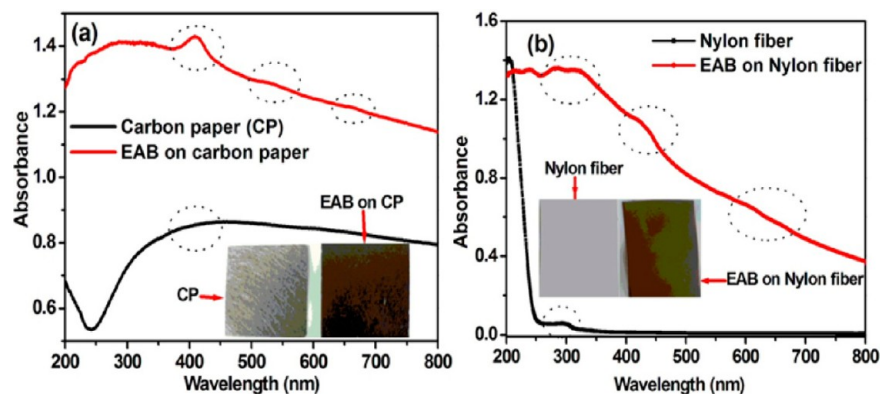


**Figure 3.** UV–visible spectra of the mixed culture EABs developed on (a) carbon paper and (b) nylon fiber for 15 days.

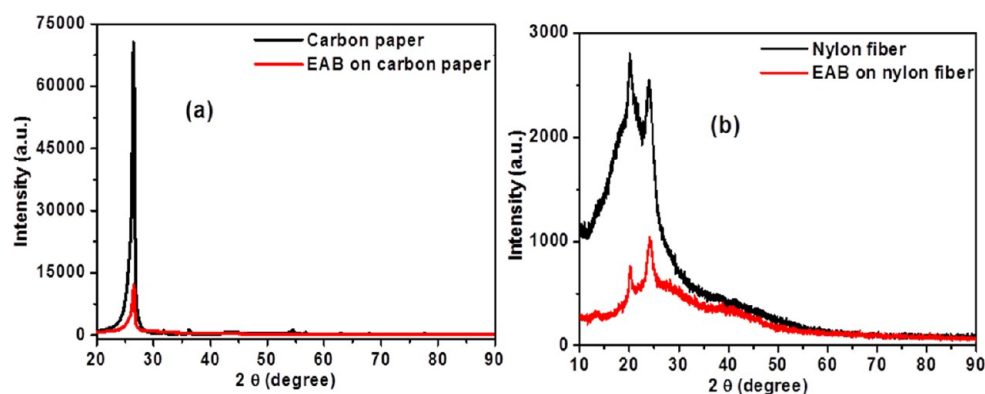


**Figure 4.** XRD patterns of mixed culture EABs formed for 15 days on (a) carbon paper and (b) nylon fiber.

fiber (Figure S5, Supporting Information), which could be due to the difference in porosity (or roughness) and the conductive nature of the support. In the case of carbon paper, the maximum absorption of pristine carbon paper was observed at  $\sim 450$  nm, which is due to the surface resonance of carbon paper.<sup>41,42</sup> The EAB developed on carbon paper showed a primary maximum absorption peak for the Soret band at  $\sim 410$  nm (Figure 3a), which is due to the  $\pi \rightarrow \pi^*$  transition in the hemeprotein present in the biofilm that indicates the oxidized form of c-Cyts. The secondary weak absorption peak at  $\sim 535$  nm ( $\beta$  band) and the very small peak at  $\sim 660$  nm ( $\alpha$  band) were observed, which are the characteristics of the reduced form of heme groups in c-Cyts (Figure 3a).<sup>39,40,43</sup> The development of EAB leads to an increase in the absorption intensity compared to the spectra of pristine carbon paper. This is because EABs contains many proteins, which cause more transitions, resulting in more intense absorption. Similarly, in the case of nylon fiber, the absorption maximum for pristine nylon fiber was observed at  $\sim 300$  nm (Figure 3b). The EAB developed on nylon fiber as support showed absorption maxima at  $\sim 300$  nm, which is due to a  $n \rightarrow \sigma^*$  transition, and an absorption peak for the Soret band at  $440$  nm (Figure 3b), which was assigned to the  $n \rightarrow \pi^*$  transition indicating the oxidized form of c-Cyts. Two very weak absorption bands were observed at  $\sim 615$  nm ( $\beta$  band) and  $\sim 655$  nm ( $\alpha$  band) due to the  $\pi \rightarrow \pi^*$  transitions, which could be assigned to the reduced form of heme groups in c-Cyts in different redox states (Figure 3b).<sup>39,40,43,44</sup> Collinson and Bowden suggested that the intensity and wavelength of the Soret absorption bands are sensitive to the conformational state of the heme groups in c-Cyts and a weakening of the heme crevice blue-shifts the Soret band further to as far as  $407$  nm.<sup>45</sup> On the other hand, the formation of a mixed high-spin/low-spin complex further blue-shifts the Soret band to  $398$ – $400$  nm; whereas the formation of a fully high-spin complex results in the appearance of the Soret band at  $395$  nm. Such shifts were observed in the Soret band of mixed culture biofilm spectra, indicating the stable and low spin conformational change in heme–protein complex of the c-Cyts in EABs.<sup>45</sup> In the case of EABs developed on carbon paper and nylon fiber, an increase in absorption intensity was observed, which was attributed to more transitions by proteins, resulting in more intense absorption. These observations confirmed the mixed culture EABs formation on different types of support and EET.

**Structural (XRD) Study of Mixed Culture EABs.** XRD is used mainly to determine the atomic and molecular structure of a crystal.<sup>46</sup> Few studies in the literature reported the use of XRD

to characterize biofilms.<sup>47,48</sup> Figure 4a and b shows the XRD patterns of mixed culture EABs formed on carbon paper and nylon fiber, respectively, for 15 days as well as the XRD patterns of carbon paper and nylon fiber only. Figure 4a and b show that the intensity of the XRD peak for carbon paper and nylon fiber from  $22$ – $28^\circ$  and  $\sim 15$ – $35^\circ$  decreased considerably, which indicates the formation of EAB on carbon paper and nylon fiber, respectively. The mixed culture EAB formation on carbon paper and nylon fiber caused changes in the incident and diffracted beam of the X-rays before and after the interaction with the support materials (carbon paper and nylon fiber). The general formula to measure the relative intensity is given by the following equation:<sup>46</sup>

$$I = I_0 |F|^2 p \left[ \frac{(1 + \cos^2 \theta)}{(\sin^2 \theta \cos \theta)} \right] e^{-2M} A(\theta) \quad (1)$$

where  $I$  is the relative integrated intensity,  $I_0$  is the incident intensity of X-ray beam,  $F$  is the structure factor,  $\theta$  is the Bragg's angle,  $A$  is the absorption factor,  $p$  is the multiplicity factor,  $e^{-2M}$  is the temperature factor, and  $\left[ \frac{(1 + \cos^2 \theta)}{(\sin^2 \theta \cos \theta)} \right]$  is the Lorentz polarization factor. From eq 1, the value of  $A$  can be written as  $A = 1/2\mu$ , where  $\mu$  is the absorption coefficient. The absorption factor in the intensity equation will be affected by the thickness of the EABs because the sample is more than that of the uncoated layer. Therefore, the absorption coefficient will increase, resulting in a decrease in intensity.<sup>46</sup> Other factors also influence the peak intensity, such as crystallinity of the specimen, change in the incident and diffracted beam, sensitivity of the detector, operating kV/mA, etc. In this study, the EAB layer formed was amorphous in nature, so crystallinity of the specimen at the surface (support) will change and the intensity of the XRD peak will be reduced. Aleksandrov et al. reported that the amorphous layer affects the incident and reflected-diffracted XRD beam, resulting in additional specular reflection and a decrease in XRD peak intensity.<sup>49</sup> The same behavior was also observed in the present study, which confirms the formation of mixed culture EABs on carbon paper and nylon fiber.

**Electrochemical Studies of EAB.** To efficiently understand the bioelectrochemical system and EET, it is important to examine redox proteins, such as c type cytochromes (c-Cyts), in viable EABs.<sup>39</sup> CV is probably the most widely used analytical tool for examining the EET process in EABs.<sup>1,2,23,29</sup> For different electrochemical studies, three sets of EABs were prepared at different time intervals i.e. one day EAB (day 1), seven days (day 7), and fifteen days (15 day). For each type of

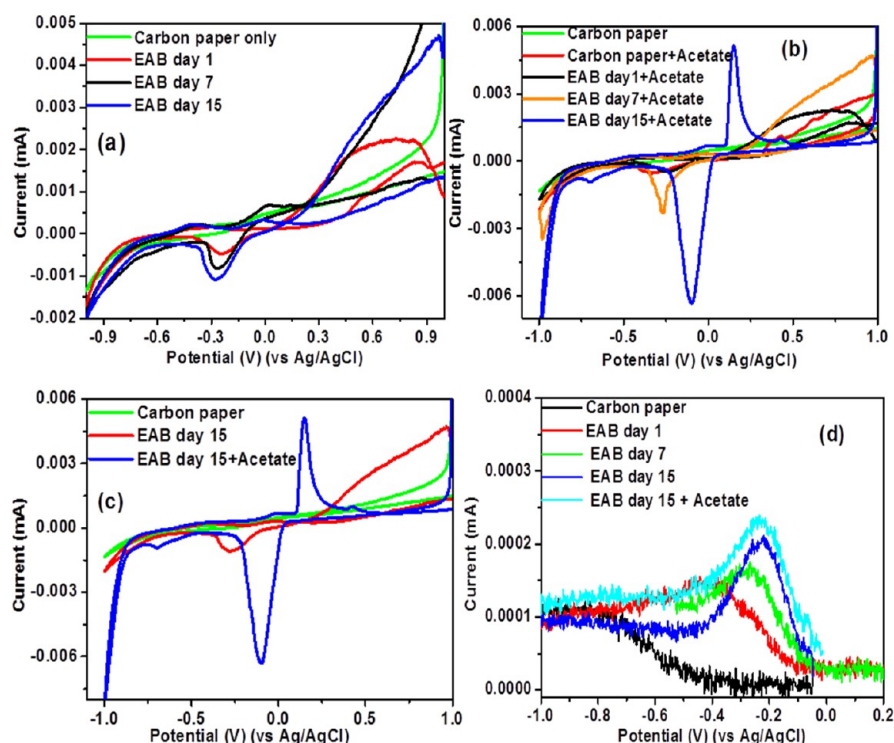


**Figure 5.** (a–c) CV of EAB developed for days 1, 7, and 15 with and without sodium acetate with a scan rate of  $1 \text{ mV s}^{-1}$ . (d) DPV of EAB developed for 1, 7, and 15 days with and without sodium acetate.

EAB, three different types of electrochemical study (CV, DPV, and EIS) were performed to determine the development of EABs, and their electrochemical response at different applied potentials with acetate and without acetate. For the control experiments, plain carbon paper was used for different types of electrochemical studies, such as CV, DPV, and EIS.

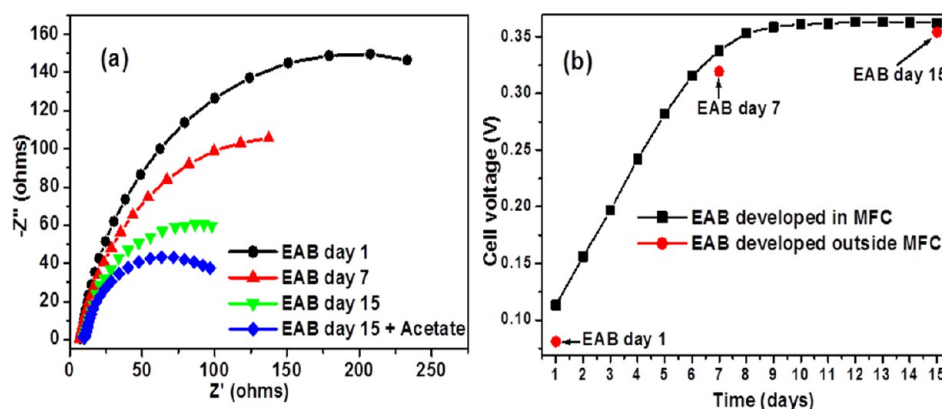
**Cyclic Voltammetry Studies of EABs.** CV was performed for the highly sensitive detection of EET. CV is used to measure the catalytic activity of EABs, but the application of CV to a living bacterial biofilm requires the limiting potential range to prevent harmful oxidation or reduction conditions with the selection of informative scan rates.<sup>18,23</sup> CV at low scan rates revealed stable catalytic features of EABs.<sup>23</sup> For the CV measurements, a slow scan rate ( $1 \text{ mV/s}$ ) was chosen because the EAMs require some time to consume the fuel (organic matter) and then produce the electrons.<sup>23</sup> Under this condition, the rate of electron transfer from the EAB to the electrode was enhanced. The CV technique can also be used to examine the rate limiting steps in current generation by EABs, and the EET occurs in EABs.<sup>7,50,51</sup> Figure 5a shows the cyclic voltammograms of EAB of 1, 7, 15 days and carbon paper only, which indicates that the current increases in proportion to the development of EAB on carbon paper. Compared to the EABs on carbon paper at different days, no redox peaks were observed before biofilm formation (Figure 5a). This confirms that the redox peaks observed in the case of EAB on 1, 7, and 15 days on carbon paper are due solely to the biofilms. The reduction current appears to be high for the EAB grown for longer duration, i.e., 15 days, because of an increase in bacterial density which enhances the number of electrons generated by oxidizing the acetate, which in turn affects the conductivity and capacity.

Figure 5b shows the cyclic voltammograms of EAB at 1, 7, and 15 days with acetate, which shows well pronounced redox

peaks for EAB on day 15 with acetate. This suggests that after the full development of EAB (day 15) with acetate, EAB generates an increasing number of electrons by biologically decomposing acetate, and the biologically produced electrons were transferred extracellularly to the electrode, which is quite fast.

Figure 5b and c shows the catalytic behavior for the bioelectrooxidation of acetate by the appearance of an oxidation and reduction peak at an onset potential of  $-0.09$  and  $0.15 \text{ V}$  during the scan. The two clear peaks in the presence of a substrate, and the lack of a peak in the absence of substrate (Figure 5b and c) indicated that the electrons had been retrieved from acetate oxidation as a result of biocatalysis. Figure 5c shows cyclic voltammograms of EAB at day 15 with and without acetate and shows an increase in current after the oxidation of acetate by the electroactive bacteria, which produces electrons after consuming acetate. Compared to carbon paper and the EAB at day 15, the redox peaks obtained for the EAB with acetate was well-defined, pronounced and showed oxidation and reduction peaks at  $-0.09$  and  $0.15 \text{ V}$ , respectively. Stable catalytic features with a high signal-to-noise ratio were observed when CV was performed at low scan rates ( $1 \text{ mV/s}$ ) for the day 15 EAB with acetate. Under these conditions, the rate of electron transfer increased rapidly at potentials  $> -0.09 \text{ V}$ , reaching a limiting current above a potential of  $0.15 \text{ V}$  (Figure 5b and c). This response, which is commonly called a “reversible catalytic wave”, indicates the continuous regeneration of electrons and EET from the biofilm to the electrode.<sup>23</sup> This improvement can be attributed to the higher active biomass within the biofilm, indicating the oxidizing power of active bacteria and EET of the mixed culture EABs. In addition, considering the current responses of the redox peaks with the substrate, it is reasonable to assume that direct EET using nanowires was the main mechanism





**Figure 6.** (a) EIS Nyquist plots of mixed culture EABs developed for 1, 7, and 15 days and the mixed culture day 15 EAB with acetate. (b) Periodical potential measurements (cell voltage versus time) of mixed culture EAB development in the MFC and outside MFC for 1, 7, and 15 days.

adopted by the EABs. These results suggest that a mixed culture bacteria with nanowires facilitated the EET between the bacteria and electrode.

**Differential Pulse Voltammetry Studies of EABs.** DPV analysis is normally used to better understand the redox behavior of EABs and is often used as a complementary technique to CV.<sup>23,52</sup> DPV can also be used to monitor biofilms nondestructively across a range of scan rates (up to 50 mV s<sup>-1</sup>) and pulse heights (up to 100 mV).<sup>23</sup> Figure 5d shows that DPV detected only one peak at  $\sim -0.4$  V for day 1 EAB and shifted toward a higher potential on the day 7 and 15 EABs at  $-0.2$  and  $-0.15$  V, respectively. Marsili et al. reported that when DPV is performed on mature biofilms, a sharp peak is observed compared to immature EABs, which increased in height with the biofilm.<sup>23</sup> Similar observations were also observed when EAB of different ages were used for the DPV studies (Figure 5d). The peak height increases with increasing age of the EABs.<sup>52,53</sup> Almost no peak was observed for the plain carbon paper, whereas a peak began appearing for the day 1 EAB and successively increased for the EABs on days 7 and 15. When the day 15 EAB was used with acetate, the peak height increased further, which indicates a faster EET.<sup>52,53</sup> DPV further confirmed the development of EAB on carbon paper, and the formation and transfer of electrons through the electroactive bacteria in the EAB.

**Electrochemical Impedance Spectroscopic Studies of EABs.** Electrochemical impedance spectroscopy (EIS) is used to examine biofilm growth, biofilm conductivity, and electron transfer mechanisms.<sup>54,55</sup> EIS is the most common alternating current method applied for the characterization of aqueous biointerfaces.<sup>23</sup> In most EIS methods, a small sinusoidal potential perturbation is applied to the sample. The frequency of this perturbation is changed in the range between a few millihertz and 10<sup>4</sup> Hz. The resulting sinusoidal current is analyzed using fast Fourier transform techniques to calculate the impedance ( $Z$ ) of the interface in the frequency domain to estimate the charge transfer resistance, diffusion at the surfaces covered by protein monolayers, charge transfer time constants, and mechanisms of EET.<sup>23,54,55</sup> Applications of EIS in microbial systems, in which the sample is studied at the open circuit potential, are numerous. Therefore, EIS is performed typically at the open circuit potentials, which reveal the electron transfer characteristics of the active cells attached to electrodes.<sup>23</sup>

Figure 6a shows comparative typical EIS Nyquist plots for EAB of days 1, 7, and 15, and EAB of days 15 with acetate. EIS

was performed at 0.0 V versus Ag/AgCl in potentiostatic mode. The impedance is expressed as a real part (plotted on the X-axis) and imaginary part (plotted on the Y-axis, which is negative) as a semicircle. Each point on the plot represents the impedance at a certain frequency. The impedance at the high frequency limit is the ohmic resistance,  $R_o$ , and the diameter of the semicircle is  $R_p$ .  $R_p$  is the polarization resistance (or charge transfer resistance or interfacial resistance) occurring at the surface of the electrode, which is affected by the kinetics of the electrode reactions. The smaller arc radius suggests a higher charge transfer efficiency.<sup>23,54–56</sup> The presence of biofilms on successive days on carbon paper reduced the charge transfer resistance. Furthermore, the charge transfer resistance was further reduced after adding acetate. Figure 6a shows that the arc radius of the day 15 EAB with acetate is smaller than that of the day 15 EAB, day 7 EAB, and in turn day 1 EAB. This suggests that the day 15 EAB with acetate has the lowest resistance, which accelerates the EET. The trend shows an increase in electron transfer with increasing number of days for EAB development, and the electron transfer further increases with the addition of acetate with day 15 EAB. This shows that the oxidation of acetate by EAB generates an increasing number of electrons, which is transferred extracellularly to the electrode.<sup>23,54–56</sup>

**Monitoring EAB Development in MFC and Outside MFC.** Both pure culture and mixed culture bacteria can be used in MFC bioanodes to generate electricity.<sup>57–59</sup> The use of a mixed culture, however, is more practical than a pure culture (single strain) because microbial communities are mixed in nature. The use of a pure culture is difficult and inconvenient because it requires many precautions and maintenance compared to a mixed culture.<sup>28–31,58,59</sup> The MFCs operated by a mixed culture generally show a higher power density than the pure cultures because pure cultures generally metabolize a limited range of organic compounds.<sup>28,29</sup> Moreover, the mixed culture bacteria can respond dynamically to the changing conditions. MFCs can be used to sense the biological oxygen demand and as a tool for examining the microbiology of EABs.<sup>59</sup> Therefore, a periodical potential measurement of EAB development during the growth phase in MFCs and EABs developed outside the MFC was monitored from which a plot of the cell voltage (V) versus time was obtained (Figure 6b). Figure 6b indicates that the growth of a microbial biofilm in the anode of MFC and outside MFC increases with time and becomes constant after a certain time. The growth of EABs was monitored in the MFCs

and outside the MFCs for 2 weeks and showed stable performance. This suggests that the biofilm in this system has essentially developed within this time frame and the EET has taken place, which was measured using the MFC. Figure 6b shows a linear increase in the potential of both EABs with respect to time. This supports the development of mixed culture EABs on carbon paper. The comparative development of EABs in the MFCs and outside the MFC under similar conditions showed similar trends of an increase in potential, which suggest that the development of EABs in the MFCs and outside the MFCs is similar. The development of EABs outside the MFC is easier, economical, and straightforward. This is why this method has been adopted to develop the EABs (outside MFC) and used for different applications.<sup>8–16</sup>

From the above studies, discussion and proposed mechanism, it can be concluded that after ~15 days of mixed culture EAB development outside the MFC, the as-developed mixed cultured EABs can produce sufficient electrons by biologically decomposing organic matter, such as acetate, to act as a reducing tool. The biologically produced electrons can be transferred extracellularly via nanowires (pili) to the electrodes, metal ions, or metal oxides for nanomaterial synthesis. From previous reports,<sup>8–16,25,26</sup> and the present study, it has been established that EAB is an effective tool for the synthesis of bioinspired nanomaterials, such as metal nanoparticles, nanocomposites, biohydrogen production, and environmental remediation.

**Stability and Reusability of EABs.** The stability and reusability of EABs were checked by running the CV, DPV, and EIS cycles for 3–4 times, which gave a similar type of spectra upon repeated use. In MFCs, the same EAB can be used several times. This shows the stability and reusability of EABs. In previous reports,<sup>8–16,25,26</sup> for the synthesis of nanoparticles and nanocomposites, the same EAB can be used more than one time for identical types of nanoparticles, and nanocomposites synthesis. The repeated use of EAB for nanomaterials synthesis can result in the deposition of as-synthesized nanomaterials on the EABs surface, which reduces the available surface area and slightly inhibits the EABs activities. This confirms that the EABs formed on carbon paper can be used more than once for different purposes, which establishes its stability and reusability.

## CONCLUSION

Microscopic, spectroscopic, and electrochemical methods (CV, DPV, and EIS) were used to examine mixed culture EABs to understand the EET phenomena of the electroactive bacteria to the carbon electrode via pili after biologically decomposing the acetate as carbon source. By choosing the appropriate techniques and conditions, these techniques can be used as nondestructive methods, and allow the in vivo determination of electron transfer from the whole cells (EABs) to electrodes under conditions that are comparable to those encountered in natural environments. The proposed methods can be applied to well-defined mixed culture EABs, as well as to complex microbial communities and can allow quantitative comparisons for the development of better microbial catalysts based on direct electron transfer between the bacteria and electrodes. The mixed culture EABs can be used as an electron source for various applications. The mixed culture EAB-mediated synthesis of nanoparticles, nanocomposites, biohydrogen production, and band gap narrowing of metal oxides provides a green chemistry approach for the efficient synthesis of a range of

bioinspired nanomaterials without any energy input. This approach can be extended to further strengthening the green approaches in nanoscience and nanotechnology.

## ASSOCIATED CONTENT

### Supporting Information

Further detailed information about UV–vis and FE-SEM of EABs developed on carbon paper and nylon fiber. TEM images of AuNPs, Au@TiO<sub>2</sub>, and Ag@TiO<sub>2</sub> nanocomposites synthesized by EABs. This material is available free of charge via the Internet at <http://pubs.acs.org>.

## AUTHOR INFORMATION

### Corresponding Author

\*Tel.: +82 53 810 2517. Fax: +82 53 810 4631. E-mail address: [mhcho@ynu.ac.kr](mailto:mhcho@ynu.ac.kr).

### Notes

The authors declare no competing financial interest.

## ACKNOWLEDGMENTS

This study was supported by Basic Science Research Program through the National Research Foundation of Korea (NRF) funded by the Ministry of Education, Science and Technology (Grant No: 2012R1A1A4A01005951).

## REFERENCES

- (1) Millo, D. Spectroelectrochemical analyses of electroactive microbial biofilms. *Biochem. Soc. Trans.* **2012**, *40*, 1284–1290.
- (2) Harnisch, F.; Rabaey, K. The diversity of techniques to study electrochemically active biofilms highlights the need for standardization. *ChemSusChem*, **2012**, *5*, 1027–1038.
- (3) Katuri, K. P.; Kavanagh, P.; Rengaraj, S.; Leech, D. Geobacter sulfurreducens biofilms developed under different growth conditions on glassy carbon electrodes: insights using cyclic voltammetry. *Chem. Commun.* **2010**, *46*, 4758–4760.
- (4) Borole, A. P.; Reguera, G.; Ringeisen, B.; Wang, Z.; Feng, Y.; Kim, B. H. Electroactive biofilms: Current status and future research needs. *Energy Environ. Sci.* **2011**, *4*, 4813–4834.
- (5) Halan, B.; Buehler, K.; Schmid, A. Biofilms as living catalysts in continuous chemical syntheses. *Trends Biotechnol.* **2012**, *30*, 453–465.
- (6) Erable, B.; Duteanu, N. M.; Ghangrekar, M. M.; Dumas, C.; Scott, K. Application of electro-active biofilms. *Biofouling: J. Bioadhesion Biofilm Res.* **2010**, *26*, 57–71.
- (7) Babauta, J.; Renslow, R.; Lewandowski, Z.; Beyenal, H. Electrochemically active biofilms: facts and fiction. A review. *Biofouling: J. Bioadhesion Biofilm Res.* **2012**, *28*, 789–812.
- (8) Kalathil, S.; Lee, J.; Cho, M. H. Electrochemically active biofilm-mediated synthesis of silver nanoparticles in water. *Green Chem.* **2011**, *13*, 1482–1485.
- (9) Khan, M. M.; Kalathil, S.; Lee, J.; Cho, M. H. Synthesis of cysteine capped silver nanoparticles by electrochemically active biofilm and their antibacterial activities. *Bull. Korean Chem. Soc.* **2012**, *33*, 2592–2596.
- (10) Khan, M. M.; Kalathil, S.; Han, T. H.; Lee, J.; Cho, M. H. Positively charged gold nanoparticles synthesized by electrochemically active biofilm—a biogenic approach. *J. Nanosci. Nanotechnol.* **2013**, *13*, 6079–6085.
- (11) Kalathil, S.; Khan, M. M.; Banerjee, A. N.; Lee, J.; Cho, M. H. A simple biogenic route to rapid synthesis of Au@TiO<sub>2</sub> nanocomposites by electrochemically active biofilms. *J. Nanopart. Res.* **2012**, *14*, 1051–1060.
- (12) Khan, M. M.; Ansari, S. A.; Lee, J.; Cho, M. H. Highly visible light active Ag@TiO<sub>2</sub> nanocomposites synthesized using an electrochemically active biofilm: a novel biogenic approach. *Nanoscale* **2013**, *5*, 4427–4435.



- (13) Khan, M. M.; Ansari, S. A.; Lee, J.; Cho, M. H. Novel Ag@TiO<sub>2</sub> nanocomposite synthesized by electrochemically active biofilm for nonenzymatic hydrogen peroxide sensor. *Mater. Sci. Eng., C* **2013**, *33*, 4692–4699.
- (14) Kalathil, S.; Khan, M. M.; Ansari, S. A.; Lee, J.; Cho, M. H. Band gap narrowing of titanium dioxide (TiO<sub>2</sub>) nanocrystals by electrochemically active biofilms and their visible light activity. *Nanoscale* **2013**, *5*, 6323–6326.
- (15) Ansari, S. A.; Khan, M. M.; Kalathil, S.; Nisar, A.; Lee, J.; Cho, M. H. Oxygen vacancy induced band gap narrowing of ZnO nanostructures by an electrochemically active biofilm. *Nanoscale* **2013**, *5*, 9238–9246.
- (16) Khan, M. M.; Lee, J.; Cho, M. H. Electrochemically active biofilm mediated bio-hydrogen production catalyzed by positively charged gold nanoparticles. *Int. J. Hydrogen Energy* **2013**, *38*, 5243–5250.
- (17) Dulon, S.; Parot, S.; Delia, M. L.; Bergel, A. Electroactive biofilms: new means for electrochemistry. *J. Appl. Electrochem.* **2007**, *37*, 173–179.
- (18) Fricke, K.; Harnisch, F.; Schröder, U. On the use of cyclic voltammetry for the study of anodic electron transfer in microbial fuel cells. *Energy Environ. Sci.* **2008**, *1*, 144–147.
- (19) Logan, B. E.; Murano, C.; Scott, K.; Gray, N. D.; Head, I. M. Electricity generation from cysteine in a microbial fuel cell. *Water Res.* **2005**, *39*, 942–952.
- (20) Han, T. H.; Khan, M. M.; Kalathil, S.; Lee, J.; Cho, M. H. Simultaneous enhancement of methylene blue degradation and power generation in microbial fuel cell by gold nanoparticles. *Ind. Eng. Chem. Res.* **2013**, *3* (52), 8174–8181.
- (21) Hossain, M. M.; Nakayama, H.; Goto, N. In vitro induction of apoptosis of developing brain cells by 5-azacytidine. *Int. J. Dev. Neurosci.* **1996**, *14*, 11–17.
- (22) Lee, J.-H.; Cho, M. H.; Lee, J. 3-Indolylacetonitrile decreases *Escherichia coli* O157:H7 biofilm formation and *Pseudomonas aeruginosa* virulence. *J. Environ. Microbiol.* **2011**, *13*, 62–73.
- (23) Marsili, E.; Rollefson, J. B.; Baron, D. B.; Hozalski, R. M.; Bond, D. R. Microbial biofilm voltammetry: direct electrochemical characterization of catalytic electrode-attached biofilms. *Appl. Environ. Microbiol.* **2008**, *74*, 7329–7337.
- (24) Barsoukov, E.; Macdonald, J. R. *Impedance spectroscopy-theory, experiment, and applications*, 2nd ed.; Wiley Interscience: Hoboken, NJ, 2005.
- (25) Kalathil, S.; Lee, J.; Cho, M. H. Gold nanoparticles produced in situ mediate bioelectricity and hydrogen production in a microbial fuel cell by quantized capacitance charging. *ChemSusChem* **2013**, *6*, 246–250.
- (26) Kalathil, S.; Khan, M. M.; Lee, J.; Cho, M. H. Production of bioelectricity, bio-hydrogen, high value chemicals and 3 bioinspired nanomaterials by electrochemically active biofilms. *Biotech. Adv.* **2013**, *31*, 915–924.
- (27) Kalathil, S.; Lee, J.; Cho, M. H. Catalytic role of Au@TiO<sub>2</sub> nanocomposite on enhanced degradation of an azo-dye by electrochemically active biofilms: a quantized charging effect. *J. Nanopart. Res.* **2013**, *15*, 1392–1397.
- (28) Kim, B. H.; Chang, I. S.; Gadd, G. M. Challenges in microbial fuel cell development and operation. *Appl. Microbiol. Biotechnol.* **2007**, *76*, 485–494.
- (29) Rittmann, B. E.; Krajmalnik-Brown, R.; Halden, R. U. Pre-genomic, genomic and post-genomic study of microbial communities involved in bioenergy. *Nat. Rev. Microbiol.* **2008**, *6*, 604–612.
- (30) Liu, Y.; Harnisch, F.; Fricke, K.; Schröder, U.; Climent, V.; Feliu, J. M. The study of electrochemically active microbial biofilms on different carbon-based anode materials in microbial fuel cells. *Biosens. Bioelectron.* **2010**, *25*, 2167–2171.
- (31) Patil, S. A.; Harnisch, F.; Koch, C.; Hübschmann, T.; Fetzer, I.; Carmona-Martínez, A. A.; Müller, S.; Schröder, U. Electroactive mixed culture derived biofilms in microbial bioelectrochemical systems: The role of pH on biofilm formation, performance and composition. *Bioresour. Technol.* **2011**, *102*, 9683–9690.
- (32) Lovley, D. R. The microbe electric: conversion of organic matter to electricity. *Curr. Opin. Biotechnol.* **2008**, *19*, 564–571.
- (33) Lovley, D. R. Live wires: direct extracellular electron exchange for bioenergy and the bioremediation of energy-related contamination. *Energy Environ. Sci.* **2011**, *4*, 4896–4906.
- (34) Malvankar, N. S.; Vargas, M.; Nevin, K. P.; Franks, A. E.; Leang, C.; Kim, B. C.; Inoue, K.; Mester, T.; Covalla, S. F.; Johnson, J. P.; Rotello, V. M.; Tuominen, M. T.; Lovley, D. R. Tunable metallic-like conductivity in microbial nanowire networks. *Nat. Nanotechnol.* **2011**, *6*, 573–579.
- (35) Malvankar, N. S.; Tuominen, M. T.; Lovley, D. R. Comment on “On electrical conductivity of microbial nanowires and biofilms”. *Energy Environ. Sci.* **2011**, *4*, 4366; *Energy Environ. Sci.* **2012**, *5*, 6247–6249.
- (36) Lovley, D. R.; Nevin, K. P. A shift in the current: new applications and concepts for microbe-electrode electron exchange. *Curr. Opin. Biotechnol.* **2011**, *22*, 1–8.
- (37) Nakamura, R.; Ishii, K.; Hashimoto, K. Electronic absorption spectra and redox properties of C type cytochromes in living microbes. *Angew. Chem., Int. Ed.* **2009**, *48*, 1606–1608.
- (38) Okamoto, A.; Nakamura, R.; Ishii, K.; Hashimoto, K. In vivo electrochemistry of c-type cytochrome-mediated electron-transfer with chemical marking. *ChemBioChem* **2009**, *10*, 2329–2332.
- (39) Jain, A.; Gazzola, G.; Panzera, A.; Zanoni, M.; Marsili, E. Visible spectroelectrochemical characterization of *Geobacter sulfurreducens* biofilms on optically transparent indium tin oxide electrode. *Electrochim. Acta* **2011**, *56*, 10776–10785.
- (40) Inoue, K.; Qian, X.; Morgado, L.; Kim, B. C.; Mester, T.; Izallalen, M.; Salgueiro, C. A.; Lovley, D. R. Purification and characterization of omcZ, an outer-surface, octaheme c-type cytochrome essential for optimal current production by *geobacter sulfurreducens*. *Appl. Environ. Microbiol.* **2010**, *76*, 3999–4007.
- (41) Singh, D. K.; Iyer, P. K.; Giri, P. K. Effect of high voltage electric pulse on microstructure of fine particles. *Nanotrends: J. Nanotechnol. Appl.* **2008**, *4*, 55–58.
- (42) Liu, H.; Nishide, D.; Tanaka, T.; Kataura, H. Large-scale single-chirality separation of single-wall carbon nanotubes by simple gel chromatography. *Nat. Commun.* **2011**, *2*, 309.
- (43) Beitlich, T.; Kühnel, K.; Schulze-Briese, C.; Shoeman, R. L.; Schlichting, I. Cryoradiolytic reduction of crystalline heme proteins: analysis by UV-Vis spectroscopy and X-ray crystallography. *J. Synchrotron Rad.* **2007**, *14*, 11–23.
- (44) Liu, Y.; Bond, D. R. Long-distance electron transfer by *G. sulfurreducens* biofilms results in accumulation of reduced c-type cytochromes. *ChemSusChem* **2012**, *5*, 1047–1053.
- (45) Collinson, M.; Bowden, E. F. UV-Visible Spectroscopy of adsorbed cytochrome c on tin oxide electrodes. *Anal. Chem.* **1992**, *64*, 1470–1476.
- (46) Cullity, B. D.; Stock, S. R. *Elements of X-ray diffraction*, 3rd ed.; Prentice Hall, 2001; Chapter 4, pp 123–157.
- (47) Florea, L. J.; Noe-Stinson, C. L.; Brewer, J.; Fowler, R.; Kearns, J. B.; Greco, A. M. Iron oxide and calcite associated with leptothrix sp. biofilms within an estavelle in the upper floridan aquifer. *Int. J. Speleol.* **2011**, *40*, 205–219.
- (48) Hu, X. B.; Xu, K.; Wang, Z.; Liding, L.; Qiangren, A. Characteristics of biofilm attaching to carriers in moving bed biofilm reactor used to treat vitamin C wastewater. *Scanning* **2013**, *35*, 283–291.
- (49) Aleksandrov, P. A.; Afanasiev, A. M.; Melkonyan, M. K.; Stepanov, S. A. X-Ray diffraction under specular reflection conditions on crystals with an amorphous surface film. *Phys. Stat. Solidi A* **1984**, *81*, 47–53.
- (50) Katuri, K. P.; Rengaraj, S.; Kavanagh, P.; Flaherty, Ö.; Leech, D. Charge transport through *geobacter sulfurreducens* biofilms grown on graphite rods. *Langmuir* **2012**, *28*, 7904–7913.
- (51) Strycharz, S. M.; Malanoski, A. P.; Snider, R. M.; Yi, H.; Lovley, D. R.; Tender, L. M. Application of cyclic voltammetry to investigate enhanced catalytic current generation by biofilm-modified anodes of

*Geobacter sulfurreducens* strain DL1 vs. variant strain KN400. *Energy Environ. Sci.* **2011**, *4*, 896–913.

(52) Marsili, E.; Baron, D. B.; Shikhare, I.; Coursolle, D.; Gralnick, J.; Bond, D. R. *Shewanella* secretes flavins that mediate extracellular electron transfer. *Proc. Natl. Acad. Sci. U.S.A.* **2008**, *105*, 3968–3973.

(53) Jain, A.; Connolly, J. O.; Woolley, R.; Krishnamurthy, S.; Marsili, E. Extracellular electron transfer mechanism in *Shewanella loihica* pv-4 biofilms formed at indium tin oxide and graphite electrodes. *Int. J. Electrochem. Sci.* **2013**, *8*, 1778–1793.

(54) Dominguez-Benetton, X.; Sevda, S.; Vanbroekhoven, K.; Pant, D. The accurate use of impedance analysis for the study of microbial electrochemical systems. *Chem. Soc. Rev.* **2012**, *41*, 7228–7246.

(55) Malvankar, N. S.; Tuominen, M. T.; Lovley, D. R. Biofilm conductivity is a decisive variable for high-current-density *Geobacter sulfurreducens* microbial fuel cells. *Energy Environ. Sci.* **2012**, *5*, 5790–95797.

(56) Ramasamy, R. P.; Ren, Z.; Mench, M. M.; Regan, J. M. Impact of initial biofilm growth on the anode impedance of microbial fuel cells. *Biotechnol. Bioeng.* **2008**, *101*, 101–108.

(57) Bond, D. R.; Lovley, D. R. Electricity production by *Geobacter sulfurreducens* attached to electrodes. *Appl. Environ. Microbiol.* **2003**, *69*, 1548–1555.

(58) Chaudhuri, S. K.; Lovley, D. R. Electricity generation by direct oxidation of glucose in mediatorless microbial fuel cells. *Nat. Biotechnol.* **2003**, *21*, 1229–1232.

(59) Chang, I. S.; Jang, J. K.; Gil, G. C.; Kim, M.; Kim, H. J.; Cho, B. W.; Kim, B. H. Continuous determination of biochemical oxygen demand using microbial fuel cell type biosensor. *Biosens. Bioelectron.* **2004**, *19*, 607–613.